Cluster Quantum Chemical ab Initio Study on the Interaction of NO Molecules with Highly Dispersed Titanium Oxides Incorporated into Silicalite and Zeolites

N. U. Zhanpeisov,*,†,‡ M. Matsuoka,† H. Yamashita,† and M. Anpo*,†

Department of Applied Chemistry, Osaka Prefecture University, 1-1 Gakuen-cho, Sakai, Osaka 599, Japan, and Boreskov Institute of Catalysis, Novosibirsk 630090, Russia

Received: March 6, 1998

Ab initio cluster quantum chemical calculations at the Hartree−Fock (HF) level have been performed for interactions of one and two NO molecules with highly dispersed titanium oxide species incorporated into silicalite (Ti−silicalite) and zeolite (Ti−zeolite) cavities. To find the similarities and differences in the adsorption mechanism, additional calculations have also been carried out on the adsorption of these and other small molecules on pure silica, alumina−silica, and titania. It was found that the NO molecule weakly adsorbs on the Ti−silicalite and Ti−zeolite while it strongly adsorbs on the titania surface. Based on the results of these calculations, different channels of NO decomposition on the Ti−silicalite or Ti−zeolite and on pure titania are discussed.

1. Introduction

Titanium oxide species containing zeolites and silicalites have been widely used as catalysts for the selective oxidation of alkenes to epoxides, of alkanes to hydroxylated products or ketones, and for hydroxylation of aromatics in the presence of hydrogen peroxide.[1−3] Since the discovery of the remarkable catalytic activity of titanium silicalites (TS-1), experimentalists and theoreticians have focused great interest on the synthesis of titanium-based molecular sieves for catalysis, to the selective oxidation of the different organic substrates on such catalysts.[1,4−6] Moreover, highly dispersed titanium oxides in zeolite or silicalite cavities were also found to exhibit unique photocatalytic activities in the reduction of CO_2 with H_2O to produce CH_3OH and the direct decomposition of NO into N_2 and O_2.[7,8] Both latter reactions are important with regard to the greenhouse effect and global air pollution control and the development of environmentally friendly technologies using solar energy.[7,9,10]

Catalytic and spectroscopic studies show that the surface Ti sites need to be isolated in the tetrahedral coordination to achieve best selectivity/activity performance, while the presence of titanium dimers or oligomers will result in inactive surface Ti sites in the octahedral coordination for the selective oxidation reactions.[1,11,12] According to UV−visible and ^{1}H solid-state NMR spectroscopy, $(OH)Ti(OSi)_3$ are the dominant framework sites while $Ti(OSi)_4$ sites are marginal at low loading.[13] Despite an increasing number of characterization studies on such modified oxides by modern experimental techniques, there are only a few theoretical studies describing the structure of the framework Ti site on Ti−silicalites and on pure titania. Thus, de Man and Sauer performed Hartree−Fock (HF) SCF structure optimizations on different substructures of titanosilicalites.[6] They showed that the typical 960 cm^{-1} vibrational band found for zeolites containing titanium can be assigned to the antisymmetric TiOSi stretching modes of the corner-sharing tetrahedra while the edge-shared TiO_4 tetrahedra are highly unlikely. Previously, such a highly unstable edge-shared structure was also predicted by Jentys and Catlow;[14] however, they found a surprisingly large Si−O bond distance at 0.199 nm. The derivation of NMR shieldings was studied by Tossel,[15] who performed HF SCF calculations on the $Ti(OH)_4$ model at the minimal MIDI basis set. The density functional theory (DFT) was used by Bernholc et al.[16] on the same model to assess the Bronsted acidity and by Millini et al.[17] also for a larger $Ti(OSi(OH)_3)_4$ cluster model. Catlow et al. showed also that the existence of the Ti−OH and Ti═$(OH)_2$-containing species are energetically more likely than the existence of the Ti═O-containing ones within the DFT level of theory.[18] Note also that a series of studies have been performed by Bredow et al. on cluster simulation of bulk properties of titania particles as rutile or anatase and their interaction with water using the semiempirical SINDO1 method.[19] However, to our knowledge no detailed theoretical studies have been performed on the interaction of NO molecules on these modified oxides within ab initio techniques.

The aim of this study is to explore the coordination of titanium in the silicalite and zeolite frameworks and to explain the different origins of the decomposition of NO on these modified oxides as compared to a pure titania surface, especially on a rutile surface, using ab initio quantum chemical calculations on molecular subunits of Ti-containing silicalites and zeolites.

2. Method of Calculation and Cluster Models

The ab initio molecular orbital calculations were performed for a series of molecules which represent substructures of silica, Ti−silicalite, Ti−zeolite, and titania (as a rutile) using Gaussian92 and Gaussian94 program packages.[20] The largest models for silica and rutile consist of a SiO_4 tetrahedron sharing its corners with four other SiO_4 tetrahedra (model I, Figure 1) and the edge-shared dititanium-containing dioctahedra surrounded by two 5-fold coordinated titanium oxides (model II, Figure 2), respectively. The other silica models correspond to the replacing of one, two, and three SiO_4 tetrahedra around the central Si atom in I by the respective number of hydroxyl groups, while for rutile, one of the 5-fold coordinated Ti sites was replaced by two water molecules in II (model IIs, Figure 3). All these models are electroneutral by their nature and satisfy their stoichiometry and boundary conditions. They can be viewed as $(MeO_2)_n(H_2O)_m$, where Me = Ti or Si and n, m are integers. Ti−silicalites can be obtained by replacing the

† Osaka Prefecture University.
‡ Boreskov Institute of Catalysis.

S1089-5647(98)01402-3 CCC: $15.00
Published on Web 08/08/1998

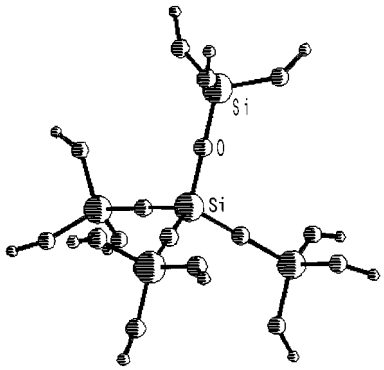

Figure 1. The silica model cluster of the composition of $H_{12}O_{16}Si_5$.

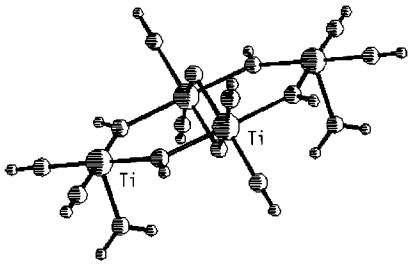

Figure 2. The titania model cluster of the composition of $H_{16}O_{16}Ti_4$.

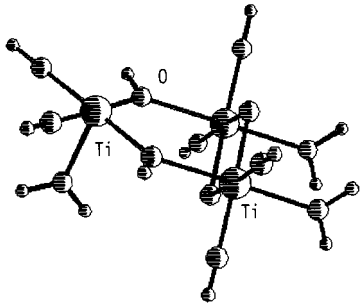

Figure 3. The smaller titania model cluster of the composition of $H_{14}O_{13}Ti_3$.

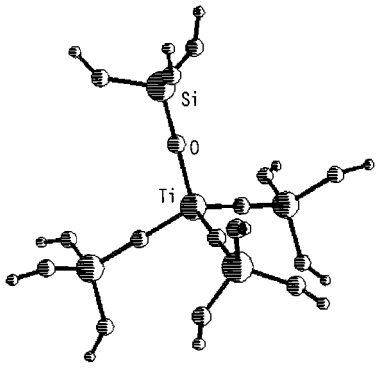

Figure 4. The Ti−silicalite model cluster of the composition of $H_{12}O_{16}Si_4Ti$.

central Si atom with Ti on the above silica clusters (model III, Figure 4), while Ti−zeolites correspond to the further substitution of one Si atom in the Ti−silicalites by Al and a proton attached to the next-neighbor basic O atom (model IV, Figure 5). Since cutting substructures from silica and zeolites generates dangling bonds, they have been saturated with hydrogen atoms to avoid boundary effects and form terminal OH groups.[21,22]

Geometry optimizations were carried out at the HF level of theory using the standard double-ζ quality LANL2DZ basis set under the following symmetry restrictions: for silica, Ti−silicalite, and Ti−zeolite models, the OTO and TOH angles

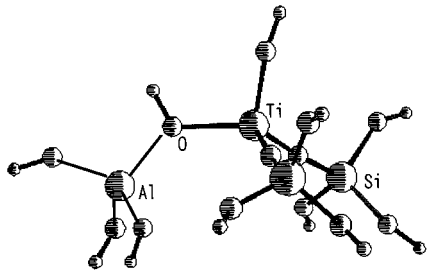

Figure 5. The Ti−zeolite model cluster of the composition of $H_{11}O_{13}AlSi_2Ti$.

where T = Si or Al in the boundary TO_4 terahedra and OH bond distances for the border H atoms were kept equal to 109.5°, 140°, and 0.0962 nm, respectively, which is in line with the generally accepted methodology for the molecular modeling of silica, alumina−silica, or zeolites.[21−23] Only the next-neighbor structural parameters which are directly responsible for NO or other molecular adsorptive interactions with these models were optimized. The open-shell structures were optimized within the restricted open-shell HF method. For all adsorption complexes considered in this study, the adsorption energy was calculated as the total energy difference between the adsorption complex and the sum of the isolated initial cluster and adsorbate molecule(s).

3. Results and Discussion

Although all of the optimized geometries for both the initial cluster models, adsorbates and their complexes considered in this study have not been presented here, they can be obtained upon request from the authors. In the following figures, only the major geometrical parameters which are directly responsible for the studied adsorption complexes are shown. Table 1 shows the energetic characteristics of both the initial cluster models and the surface adsorption complexes optimized at the HF level of theory. In addition, it also contains the corresponding data for the gas-phase NO, NO dimer, N_2O, CO, and H_2O calculated at the same level of theory.

3.1. Ti−Silicalites and Ti−Zeolites. Let us first consider the cluster models simulating the Ti−silicalites. As mentioned above, the calculations were performed for a series of molecules that represent substructures of Ti−silicalites. Table 2 shows the calculated T−O bond lengths and atomic net charges on T and O atoms in the TOSi or the TOH bridges, where T = Ti or the central Si. There is also shown the highest occupied molecular orbital (HOMO) and the lowest unoccupied molecular orbital (LUMO) energies for the silica and Ti−silicalite models together with the respective data for the Ti−zeolite modeled by the cluster of the composition of $(OH)_3Al(OH)Ti(OH)(OSi(OH)_3)_2$ (model IV-2).

We found that the optimized Ti−O bond distances in III (0.1781 nm) are in good agreement with the experimental estimations[12c,24] and larger than the Si−O distances (0.1617−0.1649 nm), which can be expected due to larger ionic radii for Ti^{4+} as compared to Si^{4+}. The TiOSi angle (179°) deviates only slightly from the linearity. When the number of hydroxyl groups bonded to the Ti atom increases, the Ti−O bond distances in TiOSi bridges further increases, while they are marginally shorter in TiOH groups. Note also that the Ti−O bond distance of the TiO(H)Al bridge in Ti−zeolite (0.1921 nm) is substantially increased due to the strong electron-acceptor ability of the $Al(OH)_3$ fragment bonded to $(OH)_2Ti(OSi(OH)_3)_2$. In going from the $Si(OSi(OH)_3)_4$ to $Si(OH)_4$ and further to the Ti−silicalite cluster models containing more hydroxyl groups

TABLE 1: Calculated Energies (E_{tot}, au) for Different Cluster Models, Surface Adsorption Complexes, and Some Molecules[a]

cluster	E_{tot}	cluster	E_{tot}	cluster	E_{tot}
I	−1224.2969	I-1···NO	−1123.8367	III-1···O[b]	−1123.1799
I-1	−994.6379	I-1···H_2O	−1070.6690	III-1···N_2O	−1232.0569
I-4	−305.6503	I-1···CO_2	−1182.2036	III-1···$(NO)_2$	−1306.7728
II	−1437.8382	II···NO	−1567.0482	IV-2···CO	−1159.9071
IIs	−1154.3855	IIs···NO	−1283.5956	IV-2···NO	−1176.4143
III	−1278.1055	IIs···CO	−1267.0971	IV-2···ON	−1176.4139
III-1	−1048.4538	IIs···H_2O	−1230.4556	IV-2···O[b]	−1121.9377
III-2	−818.8042	IIs···N_2O	−1338.0238	IV-2···N_2O	−1230.8279
III-3	−589.1513	IIs···O	−1229.1251	IV-2···$(NO)_2$	−1305.5350
III-4	−359.4975	IIs···$(NO)_2$	−1412.7252	NO	−129.1954
III-edge	−972.3510	II···$(NO)_2$	−1696.1784	CO	−112.6851
III-tio	−1048.3705	III-1···NO	−1177.6529	H_2O	−76.0109
IV-2	−1047.2131	III-1···ON	−1177.6531	N_2O	−183.5953
IV-3	−817.5688	III-1···NO[c]	−1177.5774	$(NO)_2$	−258.3142
IV-4	−587.9178	III-1···H_2O	−1124.4819	CO_2	−187.5531

[a] For the type of the cluster model see text and Figures 1−7. The number after the type of the cluster model shows how many hydroxyl groups are directly bonded to the T atom where T = Ti or the central Si. [b] Formation of the hydroperoxide group bonded to the Ti site. [c] NO adsorbs directly to the Ti site and increases its coordination number.

TABLE 2: Calculated T−O Bond Distances (R_{TO}, in nm), Atomic Net Charges on T and O Atoms (Q_T, Q_O, in e^-), and HOMO and LUMO Energies (in au) for Silica, Ti−Silicalite, and Ti−Zeolite Models, Where T = Ti or the Central Si

cluster	R_{T-O}	R_{T-OH}	Q_T	Q_{Si}	Q_O	$Q_{O(H)}$	HOMO	LUMO
I-4		0.1640	2.233			−1.028	−0.488	0.172
I-1	0.1625	0.1639	2.578	2.316	−1.312	−1.008	−0.472	0.180
I	0.1623		2.744	2.318	−1.318		−0.467	0.185
III	0.1781		2.392	2.291	−1.190		−0.468	0.087
III-1	0.1787	0.1755	2.307	2.284	−1.191	−0.950	−0.469	0.069
III-2	0.1791	0.1760	2.233	2.282	−1.193	−0.959	−0.468	0.059
III-3	0.1796	0.1766	2.153	2.280	−1.194	−0.964	−0.466	0.051
III-4		0.1770	2.078			−0.969	−0.467	0.043
IV-2	0.1759	0.1743	2.269	2.296	−1.161	−0.930	−0.382	0.049

TABLE 3: Calculated Reaction Energies (E_r, kcal/mol)[a]

reaction 1	E_r
$n = 1$	7.7
$n = 2$	14.2
$n = 3$	22.5
$n = 4$	31.6

[a] Positive values mean that the right-hand side of the reaction is the less stable form.

around the central Ti atom, one can find a monotonic decrease in the charge on the central T atom (T = Si or Ti, see Table 2). The Ti atom charge (2.39 e^-) after the Mulliken population analysis is only ca. 0.1 e^- higher as compared to the Si in III. The latter findings are somewhat opposite to the results in ref 6, in which it was found that the charge on the titanium atom is twice as large as those on the silicon atoms. The reason for this may be that in ref 6 the TiOSi angle (148.8°) strongly deviates from 180° and the charges are derived from the population analysis based on occupation numbers with multicenter corrections.[25] The increase in the number of hydroxyl groups bonded to the central Ti atom in III which were obtained by replacing the respective number of SiO_4 tetrahedra by OH groups and modeled by the following overall reactions

$$\mathrm{Ti(OSi(OH)_3)_4} + n\mathrm{H_2O} \rightarrow \mathrm{Ti(OSi(OH)_3)_{4-}}_n\mathrm{(OH)}_n + n\mathrm{Si(OH)_4} \quad (1)$$

led to a further decrease in the charge on the Ti atom and in the basicity of the O atom in the latter TiOH groups as compared to that of the TiOSi bridges. The above isodesmic reactions (1) show that they can proceed through some extra energy consumption (Table 3). According to our calculations, the formation of the first OH-containing Ti−silicalite (model III-1) was much greater as compared to the III-2, III-3, and III-4

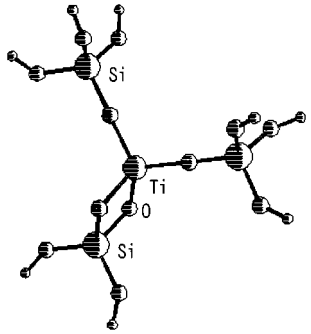

Figure 6. The strained edge-shared Ti−silicalite model.

models. Furthermore, the HOMO virtually remains the same for I and Ti−silicalite models while LUMO passes through a maximum and has a higher value for I, and it decreases for Ti−silicalite models. For Ti−zeolite both the HOMO and LUMO have relatively lower absolute values as compared to I and III (Table 2). Consequently, one can expect a higher excitation energy value for III as compared to III-1, since the direct calculation of the excited states for these models are out of the computational limits due to their large cluster size. Note also that the excitation energy value for Ti−zeolites should be lower than that of Ti−silicalites.

Formation of other strained edge-shared $=Ti(O)_2Si=$ fragments and the titanil Ti=O group containing Ti−silicalites have also been considered. They were modeled by the clusters of $((OH)_3SiO)_2Ti(O)_2Si(OH)_2$ (III-edge, Figure 6) and $((OH)_3SiO)_2$-$TiO\cdots(HO)Si(OH)_3$ (III-tio, Figure 7), respectively. The latter model can be viewed as a Ti=O group containing the Ti site of the Ti−silicalite interacting with the terminal SiOH group of the next-neighbor silica layer through the donor−acceptor bond, while the former can be obtained through the dehydroxylation of III-1 or from the decomposition of III producing III-

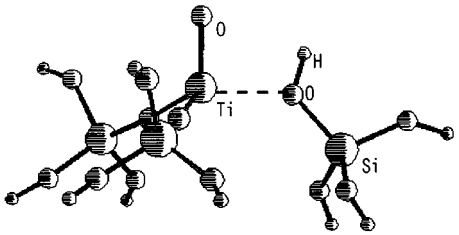

Figure 7. The Ti═O group containing Ti−silicalite model.

TABLE 4: Calculated Adsorption Energies (E_{ads}, kcal/mol)[a]

ads complex	E_{ads}	ads complex	E_{ads}
I-1···NO	2.1	III-1···NO	2.3
I-1···H_2O	12.7	III-1···ON	2.4
I-1···CO_2	7.9	III-1···NO[b]	−45.1
II···NO	9.2	III-1···H_2O	10.8
IIs···NO	9.2	III-1···N_2O	4.9
IIs···CO	16.6	III-1···$(NO)_2$	3.0
IIs···H_2O	37.1	IV-2···NO	3.6
IIs···N_2O	27.0	IV-2···ON	3.4
IIs···$(NO)_2$	16.0	IV-2···N_2O	12.2
II···$(NO)_2$	16.3	IV-2···$(NO)_2$	4.8

[a] Negative values mean that the adsorption is unprofitable. [b] NO adsorbs directly on the Ti site (see text).

edge and I-4. They can be modeled by the following overall reactions:

$$\text{III-1} \rightarrow \text{III-edge} + H_2O \quad (2)$$

$$\text{III} \rightarrow \text{III-edge} + Si(OH)_4 \quad (3)$$

$$\text{III-1} \rightarrow \text{III-tio} \quad (4)$$

Although such highly strained fragments have never been observed in ordinary Ti−zeolites, they were suggested based on EXAFS data[12c] and on the very close similarity of the Ti═O stretchings on solid surfaces to the polarized Raman and IR spectroscopy bands in solution.[26] Our calculations show that the formation of both structures on Ti−silicalites are energetically highly unprofitable. Thus, for example, the formation of the III-edge structure by reactions 2 and 3 or III-tio by reaction 4 were found to be highly endothermic, and each needs more than 50 kcal/mol extra energy (Table 1). These findings further support the conclusions of the previous quantum chemical calculations[6,14,18] and are in good agreement with the experimental data showing that such strained fragments are highly unlikely and do not exist in Ti−silicalites.

3.2. NO Molecules Adsorption. Let us now consider NO molecule adsorption on the terminal TiOH group containing Ti−silicalite models. Our attempts to localize an adsorption complex of NO on the TiOH group free of the Ti−silicalite (model III) was unsuccessfull: such an interaction was found to be unfavorable. Taking this into account, we consider NO interactions with the TiOH group involved in Ti−silicalite (model III-1) since its formation more profitable energetically as compared to the other structures.

It was found that NO adsorption proceeds through the N-end or O-end down, forming a very weak H bond (2.3 and 2.4 kcal/mol, respectively), while its adsorption directly on the Ti site is energetically highly unfavorable (Table 4, Figure 8). This is probably due to the fact that an increase in the coordination number of the Ti atom needs much more energy to distort its initial tetrahedral lattice structure. This also means that the gain in energy due to NO adsorption on the Ti site is not enough to

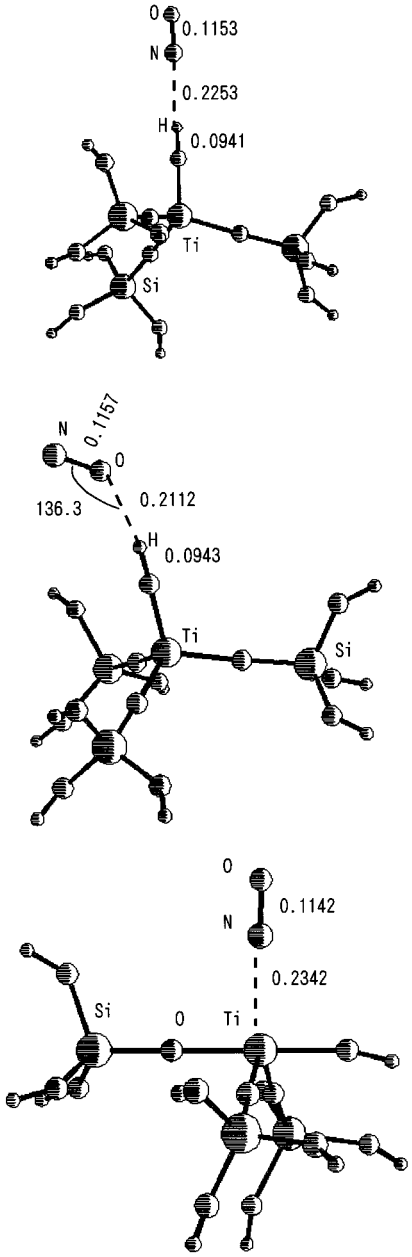

Figure 8. NO molecular adsorption on the Ti−silicalite: (a, top) the N-end down adsorption; (b, middle) the O-end down adsorption; (c, bottom) the adsorption on the Ti site via increasing its coordination state. Bond distances in nanometers and bond angle in degrees.

distort the initial lattice tetrahedral environment of the Ti−silicalite to pentacoordinated state. Probably, such transformations may occur on Ti−silicalites through interactions with adsorbate molecules with the presence of a next-neighbor additional Ti site. In that case, the possibility of forming an extraframework titania phase exists. This will be discussed later.

In going from the Ti−silicalite to Ti−zeolite, the adsorption energy of the NO molecule slightly increases (3.6 kcal/mol for the N-end down adsorption), indicating a relatively low stabilization due to a weak H bonding between the NO molecule and the acidic bridging hydroxyl group of the Ti−zeolite (Table 4, Figure 9). This stabilization value is somewhat smaller than that of the CO adsorption on the same acidic OH group of the Ti−zeolite (5.6 kcal/mol), since it involves an unpaired electron in the nonbonding orbital of the NO into its interaction with the oxide surface. Note that, as in the case of the Ti−silicalite,

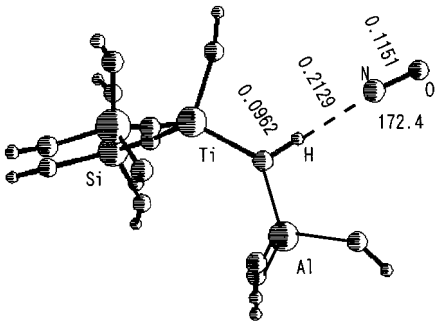

Figure 9. NO molecular adsorption on the bridging hydroxyl group of the Ti−zeolite. Bond distances in nanometers and bond angle in degrees.

only a small charge transfer (ca. 0.02 e^-) from the NO molecule to the surface and a slight decrease in the NO bond distance takes place.

Although the adsorption of CO and H_2O molecules proceed with a relatively higher gain in energy (up to 11 kcal/mol, Table 4) on these Ti−silicalite and Ti−zeolites, they adsorb even more strongly on the rutile surface due to the existence of 5-fold coordinated acidic surface Ti sites. Thus, the adsorption energies for CO and H_2O on rutile amount to 16.6 and 37.1 kcal/mol, respectively (Table 4). As a consequence, NO binds relatively stronger (9.2 kcal/mol) to the Ti site of rutile (model II) as compared to Ti−silicalite or Ti−zeolites, and its value virtually does not change when going to the smallest cluster (model IIs), indicating a local character for this type of interaction. It is also accompanied by some charge transfer from the NO to the rutile surface (0.08 e^-), and the NO bond distance is shortened by 0.0011 nm as compared to the isolated NO. There is some direct correlation between the amount of the charge transferred from the adsorbed NO to the surface on these different oxides studied: the higher its value, the stronger the adsorption.

It was considered the titania as a rutile structure instead of an anatase structure, although the latter is much more photocatalytically active than the former. The reason for this is that anatase can form three different (001), (100), and (101) stable cleavage surfaces instead of the single well-defined surface for rutile, so it leads to an increase in all calculations. Furthermore, these stable surfaces for anatase can also contain 4-fold coordinated Ti sites in addition to 5-fold coordinated sites, resulting in its high activity. Nevertheless, the above results show that NO, CO, and water molecules strongly adsorb even on a rutile surface as compared to Ti−silicalites and Ti−zeolites.

Next, we considered a two NO molecular adsorption on these modified oxide surfaces and on a rutile surface. An adsorption complex of two NO molecules on an acidic OH or Ti site of Ti−silicalite, Ti−zeolite, or rutile strongly resembles an adsorbed NO dimer in both its geometrical and electronic properties (see, for example, Figure 10). Although these adsorption complexes were found to be stable as compared to the isolated cluster and NO dimer (up to 16 kcal/mol), they are highly unstable as compared to the isolated cluster and two NO molecules. This is due to the fact that the prediction of a weak N−N bond in the NO dimer is very difficult within both standard ab initio and DFT methods.[27] Such an adsorbed NO dimer can be viewed as an intermediate of the further decomposition of NO molecules. The main difference in the decomposition products of NO molecules on the Ti−silicalite or Ti−zeolite and on titania can be explained by the different stability

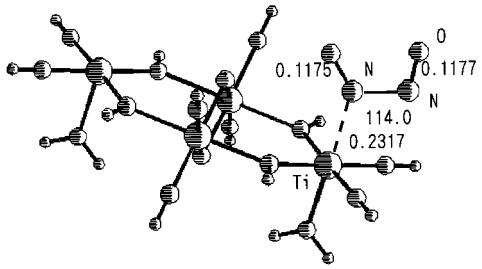

Figure 10. Two NO molecular adsorption on the 5-fold coordinated Ti site of rutile via forming a NO dimer. Bond distances in nanometers and bond angles in degrees.

TABLE 5: Calculated Reaction 6 Energies (E_r, kcal/mol)[a]

type of cluster model	E_r
IIs	−24.0
III-1	−6.4
IV-2	−11.0

[a] Negative values mean that the right-hand side of the reaction is the more stable form.

of both the adsorbed O and N_2O on these oxides which can be modeled under the following reaction:

$$Z\cdots(NO)_2 \rightarrow Z'\cdots O + Z''\cdots N_2O \qquad (5)$$

where symbols Z, Z′, and Z″ stand for the active sites on these oxide surfaces. According to our calculations, N_2O binds to the 5-fold coordinated Ti site of rutile by 27.0 kcal/mol, while its value for the Ti−silicalite and Ti−zeolite amounts only to 4.9 and 12.3 kcal/mol, respectively. Thus, on rutile, decomposition of an adsorbed NO dimer leads to the N_2O strongly adsorbed on the 5-fold coordinated Ti site while the O forms a peroxide bond with a bridging surface O atom. However, the same reaction on the Ti−silicalite and Ti−zeolite results in weakly adsorbed O and N_2O fragments. Note that, in the case of the Ti−zeolite, O will form a hydroperoxide group attached to the Ti site while N_2O forms a H bond with an acidic bridging OH group. Such interactions can be modeled by the following overall reaction for these different oxides:

$$Z + Z\cdots(NO)_2 \rightarrow Z\cdots O + Z\cdots N_2O \qquad (6)$$

The calculated reaction energies show that the reaction 6 is highly profitable in the case of rutile as compared to the Ti−silicalite or Ti−zeolite (Table 5). For this reason, we have suggested that N_2O can further interact with the O atom containing hydroperoxide group on the Ti−silicalite or Ti−zeolite leading further to its molecular decomposition products.

4. Conclusions

Ab initio molecular orbital calculations show that the NO and NO dimer weakly adsorbs on the Ti−silicalite and Ti−zeolite while it results in their relatively strong adsorption on a rutile surface. There is a direct correlation between the amount of the charge transferred from the adsorbate to the surface on these different oxides: the higher its value, the stronger the adsorption. The main difference in the decomposition products of NO molecules on the Ti−silicalite or Ti−zeolite and on titania can be explained by the differences in the stability of both the adsorbed O and N_2O.

Acknowledgment. The present work was carried out under the sponsorship of the Research Institute of Innovated Technol-

ogy for the Earth (RITE), Kyoto, which is supported by a grant from the New Energy and Industrial Technology Development Organization (NEDO), the Ministry of International Trade and Industry (MITI) of Japan.

References and Notes

(1) (a) Taramasso, M.; Perego, J.; Notari, B. U.S. Patent 4410501, 1983. (b) Notari, B. *Adv. Catal*. **1996**, *41*, 253.

(2) Sankar, G.; Rey, F.; Thomas, J. M.; Greaves, G. N. *J. Chem. Soc., Chem. Commun*. **1994**, 2279.

(3) Corma, A.; Navarro, M. T.; Peres Pariente, J. *J. Chem. Soc., Chem. Commun*. **1994**, 147.

(4) Prakash, A. M.; Kurshev, V.; Kevan, L. *J. Phys. Chem. B*. **1997**, *101*, 9794.

(5) Marchese, L.; Maschmeyer, T.; Gianotti, E.; Coluccia, S.; Thomas, J. M. *J. Phys. Chem. B*. **1997**, *101*, 8836.

(6) de Man A. J. M.; Sauer, J. *J. Phys. Chem*. **1996**, *100*, 5025.

(7) (a) Anpo, M.; Chiba, K. *J. Mol. Catal*. **1992**, *74*, 207. (b) Yamashita, H.; Ichichashi, Y.; Harada, M.; Stewart, G.; Fox, M. A.; Anpo, M. *J. Catal*. **1996**, *158*, 97. (c) Anpo, M.; Yamashita, H. In *Heterogeneous Photocatalysis*; Schiavello, M., Ed.; Wiley & Sons: London, 1997; p 131.

(8) Yamashita, H.; Ichihashi, Y.; Anpo, M.; Hashimoto, M.; Louis, C.; Che, M. *J. Phys Chem*. **1996**, *100*, 1641.

(9) Zamaraev, K. I. In *Studies in surface science and catalysis: 11th Intern. Congress on Catalysis−40th Anniversary*; Hightower, J. W., Delgass, W. N., Iglesia, E., Bell, A. T., Eds.; Elsevier Science B. V.: Amsterdam, 1996; Vol. 101, p 35.

(10) Anpo, M. *Catal. Surveys Jpn*. **1997**, *1*, 169. (b) Yoshida, S.; Takenaka, S.; Tanaka, T.; Hirano, H.; Hayashi, H. In *Studies in surface science and catalysis: 11th Intern. Congress on Catalysis−40th Anniversary*; Hightower, J. W., Delgass, W. N., Iglesia, E., Bell, A. T., Eds.; Elsevier Science B. V.: Amsterdam, 1996; Vol. 101, p 871.

(11) (a) Klein, S.; Thorimbert, S.; Maier, W. F. *J. Catal*. **1996**, *163*, 476. (b) Notari, B. *Catal. Today* **1993**, *18*, 163.

(12) (a) Deo, G.; Turek, A.; Wachs, I.; Huybrechts, D.; Jacobs, P. *Zeolites* **1993**, *13*, 365. (b) Blasco, T.; Camblor, M.; Corma, A.; Perez Pariente, J. *J. Am. Chem. Soc*. **1993**, *115*, 11806. (c) Trong On, D.; Bittar, A.; Sayari, A.; Kaliaguine, S.; Bonneviot, L. *Catal. Lett.* **1992**, *16*, 85.

(13) Le Noc, L.; Trong On, D.; Solomykina, S.; Echchahed, B.; Beland, F.; Cartier dit Moulin, C.; Bonneviot, L. In *Studies in surface science and catalysis: 11th Intern. Congress on Catalysis−40th Anniversary*; Hightower, J. W., Delgass, W. N., Iglesia, E., Bell, A. T., Eds.; Elsevier Science B. V.: Amsterdam, 1996; Vol. 101, p 611.

(14) Jentis, A.; Catlow, C. *Catal. Lett*. **1993**, *22*, 251.

(15) Tossel, J. *J. Magn. Reson*. **1991**, *94*, 301.

(16) Bernholc, J.; Horsley, J.; Murrell, L.; Sherman, L.; Soled, S. *J. Phys. Chem*. **1987**, *91*, 1526.

(17) Millini, R.; Perego, G.; Seiti, K. In *Studies in surface science and catalysis*; Weitkamp, J., Karge, H., Pfeifer, H., Hölderich, W., Eds.; Elsevier: Amsterdam, 1994; Vol. 84, p 2123.

(18) Sinclair, P. E.; Sankar, G.; Catlow, C. R. A.; Thomas, J. M.; Maschmeyer, T. *J. Phys. Chem. B* **1997**, *101*, 4232.

(19) (a) Bredow, T.; Jug, K. *Chem. Phys. Lett*. **1994**, *223*, 89. (b) Bredow, T.; Jug, K. *Surf. Sci*. **1995**, *327*, 398. (c) Jug, K.; Geudtner, G.; Bredow, T. *J. Mol. Catal*. **1993**, *82*, 171. (d) Bredow T.; Jug, K. *J. Phys. Chem*. **1995**, *99*, 285. (e) Bredow, T.; Geudtner, G.; Jug, K. *J. Chem. Phys*. **1996**, *105*, 6395.

(20) (a) Frisch, M. J.; Trucks, G. W.; Head-Gordon, M.; Gill, P. M. V.; Wong, M. W.; Foresman, J. B.; Johnson, B. G.; Schlegel, H. B.; Rob, M. A.; Replogle, E. S.; Gomperts, R.; Andres, J. L.; Raghavachari, K.; Binkley, J. S.; Gonzales, C.; Martin, R. L.; Fox, D. J.; Defrees, D. J.; Baker, J.; Stewart, J. J. P.; Pople, J. A. *GAUSSIAN92*; Gaussian Inc.: Pittsburgh, PA, 1992. (b) Frisch, M. J.; Trucks, G. W.; Schlegel, H. B.; Gill, P. M. W.; Johnson, B. G.; Robb, M. A.; Cheeseman, J. R.; Keith, T.; Petersson, G. A.; Montgomery, J. A.; Raghavachari, K.; Al-Laham, M. A.; Zakrzewski, V. G.; Ortiz, J. V.; Foresman, J. B.; Cioslowski, J.; Stefanov, B. B.; Nanayakkara, A.; Challacombe, M.; Peng, C. Y.; Ayala, P. Y.; Chen, W.; Wong, M. W.; Andres, J. L.; Replogle, E. S.; Gomperts, R.; Martin, R. L.; Fox, D. J.; Binkley, J. S.; Defrees, D. J.; Baker, J.; Stewart, J. P.; Head-Gordon, M.; Gonzalez, C.; Pople, J. A. *GAUSSIAN 94, Revision D.3*; Gaussian Inc., Pittsburgh, PA, 1995.

(21) Sauer, J.; Ugliengo, P.; Garrone, E.; Saunders, V. R. *Chem. Rev*. **1994**, *94*, 2095.

(22) Zhidomirov, G. M.; Kazansky, V. B. *Adv. Catal*. **1986**, *34*, 131.

(23) Zhidomirov, G. M.; Pelmenschikov, A. G.; Zhanpeisov, N. U.; Grebenuyk, A. *Kinet. Katal*. **1987**, *28*, 86 (translated by Plenum).

(24) Hursthouse, M.; Hossain, M. *Polyhedron* **1984**, *3*, 95.

(25) Ehrhardt, C.; Ahlrichs, R. *Theor. Chim. Acta* **1985**, *68*, 231.

(26) Huybrechts, D.; de Bruycker, L.; Jacobs, P. *Nature* **1990**, *345*, 240.

(27) (a) Duarte, H. A.; Salahub, D. R. *J. Phys. Chem. B* **1997**, *101*, 7464. (b) Ramprasad, K. C.; Hass, W. F.; Schneider, W. F.; Adams, J. B. *J. Phys. Chem. B* **1997**, *101*, 6903. (c) Magers, D. H.; Qiong, H.; Leszczynski, J. In *Proc. 6th Conference on Current Trends in Comput. Chem.;* Vicksburg, MS, 1997; p 86.